Microstructure and morphology of mechanically sulfated acid catalysts of α-Al$_2$O$_3$

T. K. Oliveira Costa^{1,2}, S. B. F. Santos^1, C. B. Silva^1, E. L. de Barros Neto^1, C. G. Pereira^1, N. L. de Freitas^2
^{1}Universidade Federal do Rio Grande do Norte, Departamento de Engenharia Química, Natal, RN, Brazil
^{2}Universidade Federal de Campina Grande, Unidade Acadêmica de Engenharia de Materiais,
Campina Grande, PB, Brazil

Abstract

This work reports the evaluation of the microstructure, morphology, and catalytic behavior of α-Al$_2$O$_3$ synthesized via combustion method for esterification reaction of oleic acid in soybean oil with ethanol to produce biodiesel. The reaction was evaluated with 2 wt% of catalyst at 160 °C for 3 h when the molar ratio of fatty acid:ethanol was 1:12. To enhance the catalytic performance of α-Al$_2$O$_3$, its sulfation was done by a different method using mechanical milling. The microcatalysts were characterized by X-ray diffraction, Fourie transform infrared spectroscopy, granulometric analysis, and scanning electron microscopy. Results showed α-Al$_2$O$_3$ as the major phase, presence of SO$_4^{2-}$ groups, the contribution of the sulfation process to morphology with reduction of agglomerates, and particle size from 18.98 to 15.30 μm. The yield of ester was enhanced from 80% (α-Al$_2$O$_3$ as a catalyst) to 93% (SO$_4^{2-}$/α-Al$_2$O$_3$ as a catalyst), which showed the milling as a fast method for synthesis of a highly efficient acid catalyst to produce biodiesel.
Keywords: catalyst, sulfation, esterification, biodiesel.

INTRODUCTION

Technological and industrial advantages have driven greater energy demand worldwide, and fossil fuels such as petroleum, natural gas, and coal are the main sources of energy used to supply this need. The extensive use of these fuels has created environmental problems such as climate change [1]. Biodiesel is a biofuel composed chemically of alkyl ester of fatty acid, produced by transesterification reaction of triglycerides or esterification reaction of fatty acids with alcohol [2]. It has become an attractive fuel alternative, as it is obtained from renewable and sustainable resources, and lower emission of carbon dioxide (CO$_2$), particulate compounds, and nitrogen oxides (NO and NO$_2$) [3]. The catalyst used in the production of biodiesel can be homogeneous or heterogeneous, with the homogeneous alkaline route the most widespread process in the industry, using sodium or potassium hydroxides. Although homogeneous catalysis has several advantages, the product purification process has a high cost and results in unwanted effluents, which need to be neutralized before disposal. In addition, homogeneous catalysts are more difficult to be regenerated and reused [4]. These problems can make biodiesel production more expensive, especially at an industrial level. Thus, a lot of research has been performed to study and develop new heterogeneous catalysts, which are more efficient, less expensive, minimize the formation of by-products, and have a less environmental impact [5].

Aluminum oxide (Al$_2$O$_3$) also known as alumina is amphoteric [6], which can be used to catalyze reactions, and its active form γ-Al$_2$O$_3$ is commonly used as a support for impregnations and surface modifications [7]. There are a variety of methods that can be used to synthesize alumina, such as supercritical drying, sol-gel, aerogel, azeotropic distillation, alkoxide hydrolysis, and template method [8]. Several studies report the use of alumina in biodiesel production. Zhang et al. [9] used γ-Al$_2$O$_3$ as support for NaAlO$_2$ (sodium aluminate) to catalyze the transesterification reaction of palm oil with methanol. Kashyap et al. [10] used γ-Al$_2$O$_3$ as a catalyst for the interesterification reaction of karanja oil. In another work [11], the transesterification reaction of soy oil with methanol was studied, using the basic catalyst KI/Al$_2$O$_3$ (alumina supported with potassium iodide). The impregnation of metal oxides has allowed increasing the efficiency of the catalysts since it modifies the surface of the materials with the addition of a binder, which can increase the acidity and the physical stability of the catalysts. These catalysts have shown high efficiency in the synthesis of esters from jatropha oil [12], and in the transesterification of cooking oil [13]. Some works have demonstrated that metal oxides are promising materials in many areas of catalysis. Liao et al. [14] studied the oxidation reaction of 5-hydroxymethylfurfural to 2,5-furandicarboxylic acid, using a catalyst with an active interface between Au-Pd alloy nanoparticles and cobalt oxide supports. The results showed an effective oxidation reaction with 95% of total conversion. A review of metal-organic frameworks (MOFs) and MOF-derived materials as catalysts was studied in order to detail the chemical composition and the structural

*@https://orcid.org/0000-0003-0473-0740

properties, such as surface area, porosity, and the dispersion of metal species on the MOF-derived support [15]. It was shown that this catalyst can be modified according to the desired applications, allowing it to be used in several organic transformations, valuable chemical synthesis, and, in the future, tandem reactions. Other works have studied and predicted similar applications [16-20].

The development of solid porous catalysts, which have an acid character, are of interest to the biofuel industries, mainly for the synthesis of biodiesel via acid esterification or transesterification. The synthesis of biodiesel via acid catalysis favors greater selectivity for the formation of the fatty acid ester, with a lower saponification index, resulting in the lowest cost of the product purification step [21]. These advantages encourage the search for new heterogeneous catalysts, which have preferably microstructural and morphological characteristics that favor mass transfer and reactivity during the reaction of conversion of fatty acid into biodiesel [22]. Chung and Park [23] studied the esterification of oleic acid with methanol in soybean oil, where the oleic acid was added into the oil in order to increase the free fatty acid reagent. In this work, zeolites were used to catalyze the reaction, and its catalytic activities with different pore structures and acidities were investigated in the conversion of oleic acid. The results showed an oleic acid conversion of 80%. Thus, this article aims to evaluate the microstructure, morphology, and catalytic behavior of α-Al_2O_3 synthesized by combustion method and its sulfated form via mechanical milling (SO_4^{2-}/α-Al_2O_3) as a new method to enhance catalytic performance for esterification reaction of oleic acid in soybean oil with ethanol to produce biodiesel.

METHODOLOGY

Materials: for the synthesis of the catalyst, the following reagents were used: aluminum nitrate nonahydrate [$Al(NO_3)_3.9H_2O$, Dinâmica, 99% purity] and urea (CH_4N_2O, Vetec, 99% purity) for the synthesis of alumina, and ammonium sulfate [$(NH_4)_2SO_4$, Dinâmica, 99.50% purity] for sulfation.

Synthesis of alumina: was carried out via a combustion reaction; urea was used as a fuel and was mixed with aluminum nitrate, which was the oxidizing reagent, at a molar ratio of 3.33:2.35 (fuel:oxidizer). The reagents were heated in a conical stainless-steel reactor, with a capacity of 100 g with electrical resistance coupled to the base of the reactor until reaching the flame formation temperature, when the combustion reaction occurred, about 15 min after the start of the process. After the end of combustion, the reaction product was obtained, which was aluminum oxide (α-Al_2O_3). The combustion reaction proceeded as follows, with an α-Al_2O_3 yield of 88%±3%:

$$2Al(NO_3)_3 + 5(NH_2)_2CO \rightarrow Al_2O_3 + 8N_2 + 5CO_2 + 10\,H_2O \quad (A)$$

Sulfation: the impregnation of the sulfate ion on the solid alumina was carried out through the dispersion in an attritor mill (HD-01/HDDM-01, Union Process). A solution of 30% (w/w) of $(NH_4)_2SO_4$ was added to α-Al_2O_3 and milled at 700 rpm for 30 min for wet impregnation [$Al_2O_3 + (NH_4)_2SO_4 + H_2O$]. The mixture was dried in a kiln (NI 1513i, Novainstruments) at 110 °C for 3 h and then calcined in a muffle furnace (3000 10P, EDG) at 600 °C for 3 h in an oxygen atmosphere. The heating rate was 5 °C/min. Thus, sulfated alumina SO_4^{2-}/α-Al_2O_3 was obtained.

Characterizations: the crystallinity of the catalyst was obtained from the X-ray diffraction (XRD) data obtained with a diffractometer (XRD 6000, Shimadzu; CuKα radiation). The crystallinity calculation was performed from the ratio between the integrated peak area for the crystalline fraction and the area for the amorphous fraction. The average crystallite size was calculated from the X-ray line broadening (D_{311}) by deconvolution of the secondary diffraction line of polycrystalline silicon (used as a standard) using the Scherrer equation [24]:

$$D_{hkl} = \frac{k.\lambda}{\beta.\cos\theta} \quad (B)$$

where k is a proportionality constant as a function of the particle's geometric shape, in this case, considered spherical (0.9-1.0), λ is the wavelength of the radiation used (1.54 Å, CuKα), and β is the full width at half maximum (FWHM) of the diffraction line. The confirmation of the SO_4^{2-} groups present on the surface of the microcatalysts was evaluated by its characteristic bands according to Fourie transform infrared (FTIR) spectra in the region of 4000-200 cm^{-1}. FTIR spectra were obtained using a spectrometer (Vertex 70, Bruker), with 4 cm^{-1} resolution and 120 scans. The granulometric analysis was performed with a laser diffractometer (Mastersize 2000, Malvern). The stability, or dispersion capacity of the catalyst in the medium, was assessed by measuring the zeta potential (SZ-100 series, Horiba Sci.). The analysis of the surface morphology of the synthesized alumina and after sulfation, SO_4^{2-}/α-Al_2O_3, was performed by scanning electron microscopy (SEM, Quanta 450 FEG, FEI). The determination of the specific surface area of the samples was performed by the nitrogen/helium adsorption method developed by Brunauer, Emmett, and Teller (BET) using an adsorptometer (Nova 3200e, Quantachrome). The adsorption/desorption isotherms were obtained by the volume of N_2 adsorbed to the material as a function of the relative pressure of the system. The pore volume and diameter were determined by the method of Brunauer, Joyner, and Halenda (BJH). The average particle size was determined by [25]:

$$D_{BET} = \frac{6}{S_{BET}.\rho} \quad (C)$$

where D_{BET} refers to the equivalent spherical diameter (nm), ϱ is the true density (g/cm³), and S_{BET} is the surface area (m²/g).

Catalyst application: the developed catalyst was tested in the esterification reaction of oleic acid in soybean oil with ethanol, in duplicate. The reactions were carried out in a 50

mL closed stainless steel reactor with a magnetic stirrer. To the soybean oil, oleic acid was added as an additive in the esterification reaction to simulate the high acidity of residual oils or animal fat. The proportion used was: 85% (w/w) of soy oil to 15% (w/w) of oleic acid. For the reactions, 10 g of the acidified soy oil was placed in contact with 6.3196 g of ethanol in the presence of 2% (w/w) of catalyst. The reaction took place at 160 ºC for a reaction time of 3 h. The stirring and heating of the system were promoted by a heating plate with magnetic stirring (C-MAG HS 7, Ika). After the esterification reaction, the samples were washed with distilled water until the catalyst was removed and subjected to centrifugation in a centrifuge (206-BL, Fanem) with a rotation of 9000 rpm for 20 min, promoting the separation of the components, ethyl esters (biodiesel) and water, by sedimentation. The products of the esterification reaction were analyzed by gas chromatography with flame detection by ionization (450GC-FID, Varian) with a stationary phase capillary column (Ultimetal 'Select Biodiesel Glycerides+RG', Varian, 15 m x 0.32 m x 0.45 μm). The detector temperature was 240 ºC, with an oven programmed for temperatures from 150 to 260 ºC, and a heating rate of 10 ºC/min. The carrier gas was H_2. For analysis, 50 mg of the samples were diluted in 5 mL of standard n-hexane UV/HPLC (Vetec, ACS grade) and then injected 1 μL of the solution into the equipment. The standard used for the quantification of ethyl ester was from Varian.

RESULTS AND DISCUSSION

XRD: the X-ray diffractograms of α-Al_2O_3 catalysts, untreated and treated with sulfated alumina (SO_4^{2-}/α-Al_2O_3) using the physical dispersion by means of the attritor mill, are shown in Fig. 1, where the presence of the stable crystalline phase α-Al_2O_3 (JCPDS file 89-7717) is observed in both diffractograms. The different intensities of the diffraction peaks were attributed to the possibility of a higher ordering or disordering caused by the stress of the formation of a new phase of Al_2O_3 in a small amount [26]. Thus, the addition of the SO_4^{2-} ion did not alter the crystalline structure of α-alumina. When synthesizing mesoporous catalysts with an ordered structure of SO_4^{2-}/α-Al_2O_3, Zhang et al. [27] also observed that the sulfation process did not interfere with the crystallinity of the alumina, with the calcination temperature having a greater influence on the crystallinity of the material. A similar result was observed by Said and El-Aal [26] when studying the sulfation process of zirconia by different metallic precursors, where characteristic peaks of the tetragonal structure of zirconia were observed for all sulfation agents.

The crystallinity values and crystallite size for the developed support and catalyst are shown in Table I. The values of crystallinity obtained were 83.4% and 84.2% and the crystallite sizes were 55.8 and 53.0 nm for the combustion reaction product (α-Al_2O_3, yield of 90%) and the catalyst (SO_4^{2-}/α-Al_2O_3), respectively.
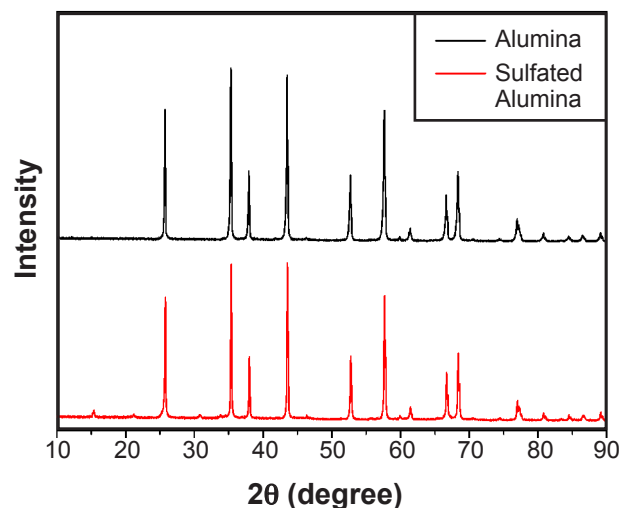
Figure 1: X-ray diffractograms of the α-Al_2O_3 and SO_4^{2-}/α-Al_2O_3 catalysts.

Despite the differences observed in crystallinity values and crystallite size of α-Al_2O_3 and SO_4^{2-}/α-Al_2O_3, these differences were small and insufficient to affirm that the sulfation process in an attritor mill favored the increase of crystallinity. The high-energy milling process, although not significant, showed a slight increase in crystallinity and a reduction in crystallite size. The observed behavior suggested the increase of the lattice strain and refinement of the grain size [28]. The slight decrease of crystallite size may occur due to comminution phenomena promoted by the high energy milling, also observed by Da Silva et al. [29], who applied the milling process for α-alumina. These authors [29], evaluating the influence of α-alumina grinding time synthesized via combustion reaction on its microstructural characteristics, observed a crystallite size of 68.5 nm and crystallinity of 89.9% for 30 min at 400 rpm. In this work, both α-alumina and the SO_4^{2-}/α-Al_2O_3 catalyst had smaller crystallite sizes than reported, indicating a lower structure agglomeration, and a crystallinity close to the range reported for ball mill processing (84.6-89.9%).

Table I - Crystallinity and crystallite size of the samples.

Characteristic	α-Al_2O_3	SO_4^{2-}/α-Al_2O_3
Crystallinity (%)	83.4	84.2
Crystallite size (nm)	55.8	53.0

FTIR: Fig. 2 shows the FTIR spectra for both microcatalysts α-Al_2O_3 and SO_4^{2-}/α-Al_2O_3 measured in the range of 4000-200 cm^{-1}. The alumina formation and the effect of the proposed sulfation process on the structure of formed α-Al_2O_3 were evaluated by FTIR measurement (Fig. 2). The broad band observed between 3800 and 3500 cm^{-1} was assigned to the O-H stretching mode, while the band at around 1663 cm^{-1} was attributed to the O-H bending frequency of water molecules [17].
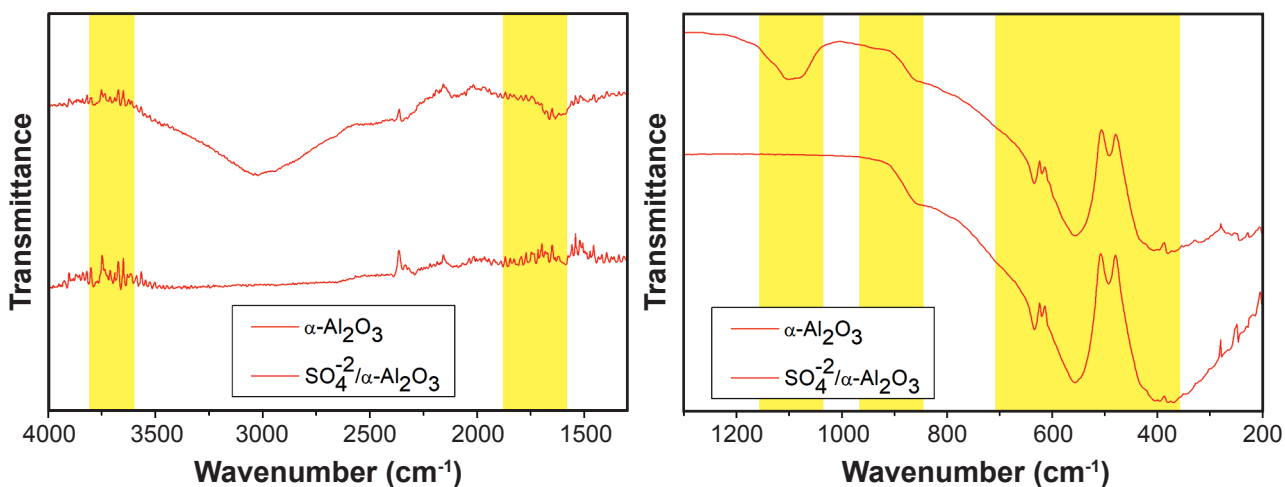
Figure 2: FITR spectra of α-Al$_2$O$_3$ and SO$_4^{2-}$/α-Al$_2$O$_3$ catalysts.

The bands observed at 1156 and 901 cm^{-1} could be assigned to the stretching of the S=O and S-O, respectively, both corresponded to the main peaks for vibration modes of the coordinated SO$_4^{2-}$ on the alumina surface, which indicated the SO$_4^{2-}$/α-Al$_2$O$_3$ formation [30]. Furthermore, the 863, 629, and 506 cm^{-1} peaks were assigned to the pseudo-boehmite structure and may confirm the α-Al$_2$O$_3$ formation [31]. Similar results were reported by: Zhang et al. [27], who studied SO$_4^{2-}$/α-Al$_2$O$_3$ synthesis via evaporation-induced self-assembly method, followed by sulfonation at different calcination temperatures; Temvuttirojn et al. [30], who studied SO$_4^{2-}$/ZrO$_2$ synthesis via precipitation method and its sulfation via impregnation with H$_2$SO$_4$; and Sajjadi et al. [31], who synthesized amorphous α-Al$_2$O$_3$ via sol-gel method.

Particle size distribution: the results of equivalent spherical diameters as a function of volume fraction for the α-Al$_2$O$_3$ and SO$_4^{2-}$/α-Al$_2$O$_3$ catalysts are observed in Fig. 3, where the obtained catalysts have a narrow agglomerates size distribution. The catalysts α-Al$_2$O$_3$ and SO$_4^{2-}$/α-Al$_2$O$_3$ resulted in agglomerates with a median diameter of 18.98 and 15.30 μm, respectively. Comparing the median size of the catalyst agglomerates without impregnation and impregnated to the α-Al$_2$O$_3$ support, a decrease of 19.39% was observed in relation to pure α-alumina; the sulfation process in the mill favored the reduction of agglomerates, justifying the increase in peak intensity observed in the XRD for the SO$_4^{2-}$/α-Al$_2$O$_3$ sample. Hao et al. [32] observed a reduction in particle size using a ball mill in wet processing of κ-Al$_2$O$_3$ and α-Al$_2$O$_3$; the materials obtained were 0.90 and 1.10 μm in size, respectively. For the investigation of the synthesis of α-Al$_2$O$_3$ from different precursors (additives and salts) using the salt smelting method, Choi et al. [33] observed particle size distributions in the range of 1.03-13 μm. The distribution curves and average particle sizes developed in this work for support and catalyst corroborated the results reported [33]. Thus, the particle size can be affected by the precursor and synthesis method, in general, resulting in microcrystalline structures.
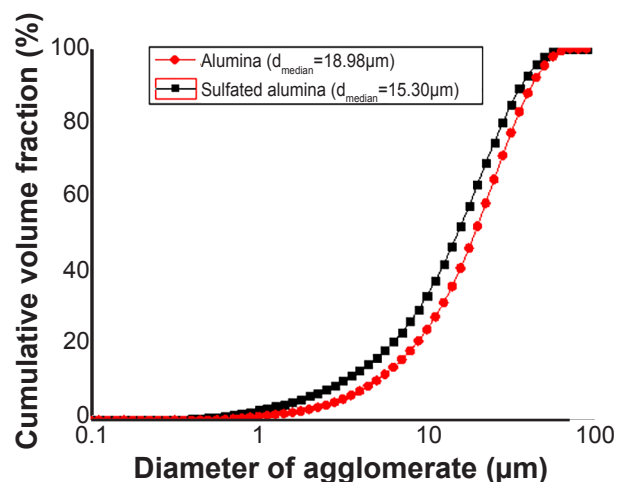
Figure 3: Particle size distribution curves of α-Al$_2$O$_3$ and SO$_4^{2-}$/α-Al$_2$O$_3$ catalysts.

SEM: Fig. 4 shows the scanning electron microscopy images of the α-Al$_2$O$_3$ and SO$_4^{2-}$/α-Al$_2$O$_3$ catalysts. The microstructures showed a greater predisposition to the formation of agglomerates for the α-alumina catalyst (Fig. 4a), while the sulfation in a mill contributed to the reduction of agglomerates observed in the catalyst SO$_4^{2-}$/α-Al$_2$O$_3$ (Fig. 4b). The images of the catalyst microstructure corroborated the average diameter observed by the particle size distribution curves of the synthesized materials. Hao et al. [32], during the development of κ-Al$_2$O$_3$, observed that physical processing in a ball mill was responsible for reducing the particle size of κ-Al$_2$O$_3$ and α-Al$_2$O$_3$. The reduction in the formation of agglomerates, observed by the morphological analysis by microscopy, corroborated the observations reported [32]. Arimatéia et al. [34] synthesized α-alumina via combustion reaction using urea as fuel, in the same conditions as the present work and observed the morphology of thin plates with irregular geometries and different sizes. Dokmai et al. [35] evaluated the effect of corrosion by distilled water
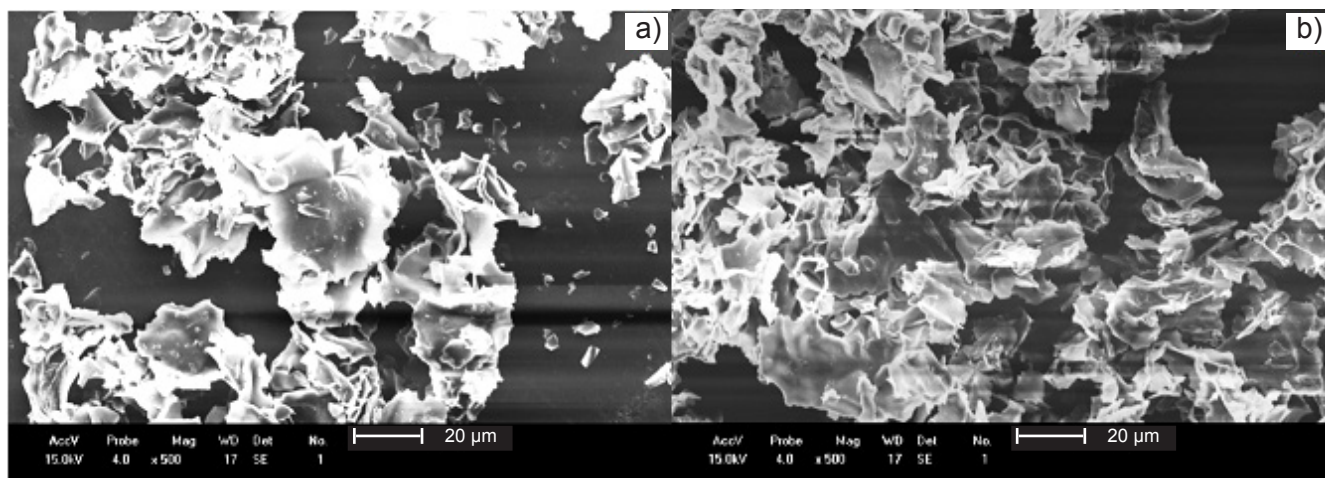
Figure 4: SEM micrographs of catalysts: a) α-Al$_2$O$_3$; and b) SO$_4{}^{2-}$/α-Al$_2$O$_3$.

of amorphous alumina between 40 and 80 °C. The authors observed that for temperatures below 40 °C, the Al-O-H group does not occur by hydrolysis and, consequently, there is no corrosion of the alumina; however, the wet method increased the interparticle porosity susceptibility, similar to the microscopy observations present in Fig. 4. The morphological and microstructural characteristics, characterized by the reduction of the size of the particles with the sulfation process in an attritor mill, make the SO$_4{}^{2-}$/α-Al$_2$O$_3$ promising for application as a catalyst in the process of esterification of vegetable oils. The reduction of agglomerates favors a larger surface area, important for the promotion of the solid-fluid interface and diffusion during the catalytic process.

Textural analysis: Table II presents the results of the textural analysis of the developed catalysts, such as the specific surface area (S$_{BET}$), particle size (D$_{BET}$), pore volume (V$_p$), and pore diameter (D$_p$). Table II shows that the impregnation process by mill dispersion (SO$_4{}^{2-}$/α-Al$_2$O$_3$) fragmented the agglomerates and consequently reduced the size of the particles, favoring the increase in surface area, particularly the SO$_4{}^{2-}$/α-Al$_2$O$_3$ catalyst compared to synthesized α-Al$_2$O$_3$. On the other hand, the pore diameter of the microstructures was not changed significantly with the processing carried out, being in the range of 3.34 to 3.36 nm, while the mesoporous volume varied between 0.005-0.007 cm^3/g. Mohebbi et al. [36] report that the ZSM-5 zeolite sulfation process did not vary the diameter or volume of the nanocatalyst mesopores, remaining in the ranges of 2.08-2.13 nm and 0.05-0.06 cm^3/g, respectively. For the developed microcatalysts SO4C and SO4M, when compared to the α-Al$_2$O$_3$, pore diameter and volume ranges of 3.34-3.36 nm and 0.005-0.007 cm^3/g, respectively, were observed, in agreement with the sulfated catalysts reported in the literature. Chiang et al. [37] prepared the catalyst SO$_4{}^{2-}$/ZrO$_2$/Al$_2$O$_3$ using H$_2$SO$_4$ as a sulfation agent, aiming at the esterification of soybean oil; they reached a surface area of 1.1 m^2/g and a pore volume of 0.00147 cm^3/g, the

material having 97% mesopores and 3% macropores. The SO4C and SO4M samples stand out for their potential application in the heterogeneous catalysis of soybean oil because they had a high surface area (3.21 and 13.60 m^2/g, respectively) and pore volume (0.005 and 0.007 cm^3/g, respectively) than those reported in the literature, which favors the contact between the active catalyst sites and the reagents.

Table II - Specific surface area (S$_{BET}$), particle size (D$_{BET}$), pore volume (V$_p$), and pore diameter (D$_p$) of the samples α-Al$_2$O$_3$ and mill impregnated SO$_4{}^{2-}$/α-Al$_2$O$_3$.

Sample	S$_{BET}$ (m^2/g)	D$_{BET}$* (nm)	V$_p$ (cm^3/g)	D$_p$ (nm)
α-Al$_2$O$_3$	3.21	0.48	0.005	3.36
SO$_4{}^{2-}$/α-Al$_2$O$_3$	13.60	0.11	0.007	3.34

* *equivalent spherical diameter.*

Catalyst application: the catalyst SO$_4{}^{2-}$/α-Al$_2$O$_3$ was used in the esterification reaction of soybean oil, via ethyl route with molar ratio fatty acid:alcohol of 1:12, in the presence of 2% catalyst at 160 °C for 3 h with magnetic stirring. The sample was centrifuged to separate the components and taken to gas chromatography to analyze the concentration of ester, monoglycerides, diglycerides, and triglycerides (Fig. 5). These results show that the amount of unreacted triglycerides in the blank and unmodified alumina were much higher than in the case of sulfated alumina, justifying further the catalyst sulfation performance in the reaction efficiency. The reactions were done in triplicate and all the results indicated this great conversion even without a catalyst; perhaps, operating conditions were responsible, such as temperature. The amount of residual oleic acid was analyzed. The final yield of ester was 93.4%, compared to the yield of 70.7% of the reaction without catalyst and 80.3% of the reaction with unmodified alumina; it was evident that the sulfation of the catalyst was efficient for the production of biodiesel, with

the potential to be studied in a future work under different operating conditions of temperature, reaction time, percentage of catalyst, and also using different alcohols. The $SO_4^{2-}/\alpha\text{-}Al_2O_3$ catalyst showed a morphology with less agglomeration and smaller particles, which would indicate a greater potential for dispersion in a medium and a higher contact of the catalysts' surface with the reagents, which also tends to promote a greater catalytic conversion of organic compounds due to SO_4^{2-} acidic character [26, 27].
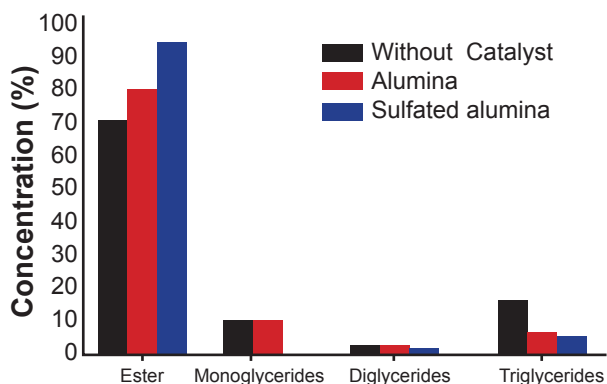
Figure 5: Yields of ester formed and residual concentrations of unreacted triglycerides of the esterification reactions without catalyst and with unmodified alumina and sulfated alumina.

Similar results were attained by Silveira Junior et al. [38], which synthesized a heterogeneous catalyst based on K_2CO_3 supported on $\gamma\text{-}Al_2O_3$ for biodiesel production by transesterification reaction from sunflower oil and ethanol. The transesterification reaction was carried out for 4 h using 5 wt% of the catalyst and different molar ratios of oil:alcohol. For the lowest content of K_2CO_3 (15% K_2CO_3/85% $\gamma\text{-}Al_2O_3$), oil:alcohol molar ratio of 1:12, and reaction temperature of 80 °C, 78.75% of yield was achieved. $\gamma\text{-}Al_2O_3$ without any impregnation method

usually shows a yield conversion of oil of around 70-80% [38]. Besides the potential of $\gamma\text{-}Al_2O_3$ powder catalysts on transesterification reactions, different methods of impregnation, as the sulfation process by mechanical milling reported in this work, are essential to reduce agglomeration problems that affect the catalytic activity. Abdeldayem et al. [39] evaluated hollow microspheres of $\gamma\text{-}Al_2O_3$ [Al(HSP)] and graphene oxide-alumina composite [GOxAl(HSP), x in wt% of the solid form prepared] for transesterification reaction of sunflower oil with methanol for biodiesel production. The composite with 5 wt% GO loading exhibited the best catalytic activity, giving an oil conversion of 97% by using 1.0 wt% catalyst to oil at 120 °C in autoclave reactor, with methanol to oil molar ratio of 30:1, and reaction time of 2 h [39]. Despite the fact that a high yield of biodiesel (97%) was reported, an autoclave reactor with a pressure of ~3 MPa, which consists of high demand energy to control the system, besides the high necessary amount of methanol (molar ratio oil:alcohol 1:30) were used. Our work allows a reaction system for a high yield (93.4%) using a molar ratio oil:alcohol 1:12, which requires less reactant, and the ethanol used is less toxic. For comparison, recent studies on the esterification/ transesterification of different oils using catalysts based on alumina are summarized in Table III. As reported, the reaction of oil into biodiesel using catalysts based on alumina presents a conversion between 70-99%. According to this table, the sulfated α-alumina ($SO_4^{2-}/\alpha\text{-}Al_2O_3$) synthesized in this study exhibited more activity for conversion than a single-phase alumina catalysts ($\alpha\text{-}Al_2O_3$ and $\gamma\text{-}Al_2O_3$) [43, 49], which indicates the performance increase due to the presence of SO_4^{2-} potential acid sites. The results of performance were satisfactory (80.3% for $\alpha\text{-}Al_2O_3$ and 93.4% for $SO_4^{2-}/\alpha\text{-}Al_2O_3$ catalyst) compared to reported studies.

Table III - Reactions using alumina as a catalyst to produce biodiesel.

Oil and alcohol	Catalyst	Maximum conversion (%)	Ref.
Waste cooking oil+methanol	γ-alumina+coconut chaff	93.84	[40]
Vegetable oil+methanol	Alumina+KI	97.70	[41]
Waste cooking oil+methanol	Alumina+sulfated zirconia	93.50	[42]
Karanja oil+methyl acetate	γ-alumina	70	[43]
Rubber seed oil+methanol	Alumina+CaO+KI	91.60	[44]
Canola oil+methanol	KOH+carbonated alumina+calcium oxide	96.30	[45]
Waste cooking oil+methanol	K/Fe$_2$O$_3$/γ-alumina	99	[46]
Waste cooking oil+methanol	γ-alumina+KOH, LiNO$_3$, NaOH	99	[47]
Waste cooking oil+methanol+acetone	Alumina+CaCO$_3$	97.98	[48]
Palm oil+methanol	γ-alumina+CaO	90.11	[49]
Non-edible oil+methanol	Alumina+molybdenum	80.90	[50]
Soybean oil+oleic acid+ethanol	α-alumina	80.3	This study
	Sulfated α-alumina	93.4	

CONCLUSIONS

A high crystalline and monophasic α-Al_2O_3 powder was synthesized by a combustion method, with an average particle size of 18.98 and 15.30 μm, for α-Al_2O_3 and SO_4^{2-}/α-Al_2O_3, respectively. The sulfation process was applied to prepare a high-performance SO_4^{2-}/Al_2O_3 for esterification reaction of soybean oil to ethyl esters; the yield of ester was enhanced from 80% (α-Al_2O_3 as a catalyst) to 93% (SO_4^{2-}/α-Al_2O_3 as a catalyst). It was evident that the sulfation of the catalyst in an attritor mill assisted to reduce the particle agglomerates, and the SO_4^{2-}/α-Al_2O_3 catalyst was highly efficient for the production of biodiesel, with the potential to be studied in future work under different operating conditions.

ACKNOWLEDGEMENTS

REFERENCES

[1] V.K. Mishra, R. Goswami, Biofuels **9**, 2 (2017) 273.

[2] J. Zhang, J. Liu, X. Huang, S. Choi, R. Zhu, S. Tang, J.Q. Bond, L.L. Tavlarides, Fuel **268** (2020) 117359.

[3] S.H.Y.S. Abdullah, N.H.M. Hanapi, A. Azid, R. Umar, H. Juahir, H. Khatoon, A. Endut, Renew. Sustain. Energy Rev. **70** (2017) 1040.

[4] F.P. de Sousa, G.P. dos Reis, C.C. Cardoso, W.N. Mussel, V.M.D. Pasa, J. Environ. Chem. Eng. **4** (2016) 1970.

[5] J.P.C. Evangelista, A.D. Gondim, L.D. Souza, A.S. Araujo, Renew. Sustain. Energy Rev. **59** (2016) 887.

[6] S.-J. Park, M.-K. Seo, Interface Sci. Technol. **18** (2011) 431.

[7] N.V. Obraztsov, D.I. Subbotin, E.A. Pavlova, V.Y. Frolov, V.L. Belyaev, Mater. Today Proc. **30**, 3 (2020) 528.

[8] P. Zhu, P. Tian, Y. Liu, H. Pang, W. Gong, J. Ye, G. Ning, Micropor. Mesopor. Mat. **292** (2020) 109752.

[9] Y. Zhang, S. Niu, C. Lu, Z. Gong, X. Hu, Energy Convers. Manag. **203** (2020) 112263.

[10] S.S. Kashyap, P.R. Gogate, S.M. Joshi, Chem. Eng. Process. Process Intensif. **136** (2019) 11.

[11] W. Xie, H. Li, J. Mol. Catal. A Chem. **255** (2006) 1.

[12] A. Ramesh, K. Palanichamy, P. Tamizhdurai, S. Umasankar, K. Sureshkumar, K. Shanthi, Mater. Lett. **238** (2019) 62.

[13] B.R. Vahid, N. Saghatoleslami, H. Nayebzadeh, J. Toghiani, J. Taiwan Inst. Chem. Eng. **83** (2018) 115.

[14] Y.-T. Liao, N.V. Chi, N. Ishiguro, A.P. Young, C. Tsung, K.C.-W. Wu, Appl. Catal. B **270** (2020) 118805.

[15] H. Konnerth, B.M. Matsagar, S.S. Chen, M.H.G. Prechtl, F.-K. Shieh, K.C.-W. Wu, Coord. Chem. Rev. **416** (2020) 213319.

[16] Y.-T. Liao, B.M. Matsagar, K.C.-W. Wu, ACS Sustain. Chem. Eng. **6**, 11 (2018) 13628.

[17] E. Doustkhah, J. Lin, S. Rostamnia, C. Len, R. Luque, X. Luo, Y. Bando, K.C.-W. Wu, J. Kim, Y. Yamauchi, Y. Ide, Chem. Eur. J. **25** (2019) 1614.

[18] C.-C. Chueh, C.-I. Chen, Y.-A. Su, H. Konnerth, Y.-J. Gu, C.-W. Kung, K.C.-W. Wu, J. Mater. Chem. A **7** (2019) 17079.

[19] C.-C. Lee, C.-I. Chen, Y.-T. Liao, K.C.-W. Wu, C.-C. Chueh, Adv. Sci. **6** (2019) 1801715.

[20] J. Wang, Y. Xu, B. Ding, Z. Chang, X. Zhang, Y. Yamauchi, K.C.-W. Wu, Angew. Chem. Int. Ed. **57**, 11 (2018) 2894.

[21] F. Peng, Y. Jiang, J. Feng, L. Li, H. Cai, J. Feng, J. Eur. Ceram. Soc. **40**, 6 (2020) 2480.

[22] J.C. Védrine, Chinese J. Catal. **40**, 11 (2019) 1627.

[23] K. Chung, B. Park, J. Ind. Eng. Chem. **15** (2009) 388.

[24] F.R. Feret, Analyst **123** (1998) 595.

[25] J.S. Reed, *Principles of ceramics processing*, John Wiley Sons, New York (1996).

[26] A.E.A. Said, M.A. El-Aal, J. Fuel Chem. Technol. **46**, 1 (2018) 67.

[27] Z. Zhang, H. Yuan, Y. Wang, Y. Ke, J. Solid State Chem. **280**, 1 (2019) 1.

[28] J.F. Silva, U.U. Gomes, E.O. Almeida, A.S. Silva, G.B. Pinto, C.P. Souza, Mater. Sci. Forum **730** (2013) 385.

[29] M.C. da Silva, N.C.O. Costa, D.S. Lira, J. Dantas, A.C.F.M. Costa, N.L. De Freitas, Mater. Sci. Forum **820**, 1 (2015) 155.

[30] C. Temvuttirojn, N. Chuasomboon, T. Numpilai, K. Faungnawakij, M. Chareonpanich, J. Limtrakul, T. Witoon, Fuel **241** (2019) 695.

[31] S.A. Sajjadi, N.P. Ahmadi, S. Yazdani, Surf. Coat. Technol. **405** (2020) 126546.

[32] Z. Hao, B. Wu, T. Wu, Ceram. Int. **44**, 7 (2018) 7963.

[33] J. Choi, S.W. Lee, Y.H. Kima, Ceram. Int. **46**, 9 (2020) 13233.

[34] R.R. Arimatéia, R.B.L. Hanken, A.D.B. Oliveira, P. Agrawal, N.L. Freitas, E.S. Silva, E.N. Ito, T.J.A. Melo, J. Thermoplast. Compos. Mater. **34** (2021) 451.

[35] V. Dokmai, R. Methaapanon, V. Pavarajarn, Appl. Surf. Sci. **499** (2020) 143906.

[36] S. Mohebbi, M. Rostamizadeh, D. Kahforoushan, Micropor. Mesopor. Mat. **294** (2019) 109845.

[37] C. Chiang, K. Lin, C. Shu, J.C. Wu, K.C. Wu, Y. Huang, Catal. Today **348** (2019) 257.

[38] E.G. Silveira Junior, V.H. Perez, I. Reyero, A. Serrano-Lotina, O.R. Justo, Fuel **241** (2019) 311.

[39] H.M. Abdeldayem, B.G. Salib, F.I. El-Hosiny, Fuel **277** (2020) 118106.

[40] A.S. Yusuff, J.O. Owolabi, S. Afr. J. Chem. Eng. **30** (2019) 42.

[41] J.P.C. Evangelista, A.D. Gondim, L.D. Souza, A.S. Araujo, Renew. Sustain. Energy Rev. **59** (2016) 887.

[42] B.R. Vahid, N. Saghatoleslami, H. Nayebzadeh, J. Toghiani, J. Taiwan Inst. Chem. Eng. **83** (2018) 115.

[43] S.S. Kashyap, P.R. Gogate, S.M. Joshi, Chem. Eng. Process. Process Intensif. **136** (2019) 11.

[44] Z.K.A. Razak, S.H. Kamarullah, S.N.M. Khazaai, G.P. Maniam, Malaysian J. Anal. Sci. **22**, 2 (2018) 279.

[45] H. Nayebzadeha, M. Haghighib, N. Saghatoleslamia, M. Tabasizadehd, S. Yousefib, Energy Convers. Manag. **171** (2018) 566.

[46] F. Yazdani, M. Akia, F. Khanbolouk, H. Hamze, H. Arandiyan, Biofuels **2019** (2019) 1759.

[47] F. Khanbolouk, M. Akia, H. Arandiyan, F. Yazdani, Y.

Dortaj, J. Nanostruct. Chem. **7** (2017)191.

[48] V. Singh, M. Yadav, Y.C. Sharma, Fuel **203** (2017) 360.

[49] B.K. Uprety, W. Chaiwong, C. Ewelike, S.K. Rakshit, Energy Convers. Manag. **115** (2016) 191.

[50] Q. Zhang, F. Wei, P. Ma, Y. Zhang, F. Wei, H. Chen, Waste Biomass Valori. **9** (2018) 911.